

## Article

# Potential Use of Microbially Induced Calcite Precipitation for the Biocementation of Mine Tailings

Héctor Zúñiga-Barra <sup>1</sup>, Eduardo Ortega-Martínez <sup>1</sup>, Javiera Toledo-Alarcón <sup>2</sup> , Álvaro Torres-Aravena <sup>1</sup>, Lorena Jorquera <sup>3</sup>, Mariella Rivas <sup>4</sup>  and David Jeison <sup>1,\*</sup> 

<sup>1</sup> Escuela de Ingeniería Bioquímica, Pontificia Universidad Católica de Valparaíso, Av. Brasil 2085, Valparaíso 2362803, Chile

<sup>2</sup> Facultad de Ingeniería y Ciencias, Universidad Adolfo Ibáñez, Av. Padre Hurtado 750, Viña del Mar 2520000, Chile

<sup>3</sup> Escuela de Ingeniería en Construcción, Pontificia Universidad Católica de Valparaíso, Av. Brasil 2147, Valparaíso 2362804, Chile

<sup>4</sup> Laboratorio de Biotecnología Ambiental Aplicada, Departamento de Biotecnología, Facultad de Ciencias del Mar y Recursos Biológicos, Universidad de Antofagasta, Av. Angamos 601, Antofagasta 1270300, Chile

\* Correspondence: david.jeison@pucv.cl

**Abstract:** Mining activities offer clear economic benefits for mineral-rich countries. However, mining operations can produce several environmental impacts. Many of these are associated with generating and managing mining waste known as tailings, which are typically stored in surface facilities. Windblown dust emissions from tailing deposits can cause severe damage to local ecosystems and adverse health effects for the surrounding population. Microbially induced calcite precipitation (MICP) can be used for the superficial biocementation of tailings, thereby preventing such emissions. This research studied the capacity of MICP for the biocementation of tailings. The effect of applying different doses of biocementation reagents and two different methods for their application were evaluated. Results show that a relevant increase in surface strength can be achieved, especially if reagents are mechanically mixed with the tailings to induce a more homogeneous distribution of precipitates. Micrographical and mineralogical analysis by SEM, FTIR and XRD analysis showed the precipitation of calcium in the form of anorthite, calcite or vaterite. Overall results indicate that calcite precipitation can be induced in tailing by microorganisms with urease activity, providing a potential technique for the biocementation of this material.

**Keywords:** Microbially induced calcite precipitation; tailing; biocementation; calcium carbonate; *Sporosarcina pasteurii*



**Citation:** Zúñiga-Barra, H.; Ortega-Martínez, E.; Toledo-Alarcón, J.; Torres-Aravena, Á.; Jorquera, L.; Rivas, M.; Jeison, D. Potential Use of Microbially Induced Calcite Precipitation for the Biocementation of Mine Tailings. *Minerals* **2023**, *13*, 506. <https://doi.org/10.3390/min13040506>

Academic Editors: Wentao Hu and Hong Peng

Received: 7 March 2023

Revised: 24 March 2023

Accepted: 26 March 2023

Published: 1 April 2023



**Copyright:** © 2023 by the authors. Licensee MDPI, Basel, Switzerland. This article is an open access article distributed under the terms and conditions of the Creative Commons Attribution (CC BY) license (<https://creativecommons.org/licenses/by/4.0/>).

## 1. Introduction

Mineral resource-rich nations face significant challenges when coupling economic growth with long-term inclusive and sustainable development [1,2]. Mining operations result in the simultaneous production of valuable mineral commodities and a vast volume of waste by-products that must be managed [3]. Tailings represent the main waste stream commonly deposited in surface tailing storage facilities (TSF), usually using dams [3]. Tailing storage facilities require enormous extensions of land, are virtually devoid of vegetation during their active state, and are exposed to environmental conditions [4].

Mine tailing may present low cohesion, loose structure and a small particle size distribution. Moreover, wind-induced shear stresses can lead to windblown dust emissions (WDE) into the atmosphere [4,5]. These emissions can cause damage to local ecosystems and severe health problems for people living in the surrounding areas. Indeed, WDE can mobilize dangerous levels of hazardous elements, such as Cd, Cr and As. Furthermore, exposure to these elements can reduce nervous system functions and, in the long term, lead to degenerative diseases such as Alzheimer's, Parkinson's and others [6,7].

Several alternatives have been proposed to address WDE from tailing deposits. The most commonly reported methods are the application of surface penetrants, surface covers, and the use of vegetation covers [4,8–10]. However, these treatments are often expensive and complex due to the large surface areas involved. Moreover, they present particular difficulties or limitations. For example, surface penetration methods, such as irrigation, are less viable in arid and semi-arid areas, as they favor rapid water evaporation and only provide a temporary treatment of a few hours [11,12]. In addition, when wet soils are exposed to high wind speeds ( $6\text{--}9\text{ m s}^{-1}$ ), dust emissions are similar to those for dry soils [13]. On the other hand, methods involving surface cover or phytoremediation are more likely to be applied in the case of inactive TSF or those that have already reached their capacity. Therefore, despite the alternatives already commented on, there is still a need to develop affordable, effective, and sustainable technologies to control dust emissions from TSF [4].

Biogeochemical processes are creating increasing interest as a potential tool to modify several properties of soil, such as density, porosity and saturation [14,15]. Compared with traditional methods, biogeochemical processes have been regarded as a more affordable alternative with a lower environmental impact [16]. Microbially induced calcite precipitation (MICP) is most likely the most studied biogeochemical process that has the potential to improve soil mechanical properties such as shear strength and stiffness [14,15].

MICP promotes calcium carbonate precipitation as a result of biological activity, which can be induced by a wide variety of microorganisms through different metabolic pathways. However, the most reported alternative is MICP driven by ureolytic activity [17,18]. In ureolytic-driven MICP,  $\text{CaCO}_3$  precipitation is induced by urease-producing microorganisms that catalyze the hydrolysis of urea, a phenomenon that is described in the following reactions [19,20]:



MICP requires the combined addition of a source of calcium, urea and an ureolytic-active microorganism. As a result of the ureolytic activity, urea is hydrolyzed into carbonate and ammonium [21]. The latter produces an alkalization of the environment, promoting the binding of calcium and carbonate and further  $\text{CaCO}_3$  precipitation [22].

MICP has been proposed as a method for creating impermeable barriers, reducing soil liquefaction, and controlling dust emissions [23–25]. During surface treatment of soils by MICP, the produced  $\text{CaCO}_3$  creates bridges between soil particles, increasing the bearing capacity of the soil and resulting in the formation of a crust over the biocemented material, which increases the strength of the surface to wind erosion [26–28].

So far, the potential of MICP as a tool for the control of WDE has mainly been tested through research conducted on sand and silty sand. On those soils, results indicate that MICP treatment can, depending on the conditions, completely prevent WDE [26,28–31]. However, to date, only a few reports are available dealing with MICP application on mine tailing [4,23,27,32–35]. Tailing may represent a complex material for MICP application due to its physicochemical characteristics, which vary considerably depending on geographical location, the type of ore extracted and the applied mineral processes [18,36]. Considering the already identified potential of MICP as a useful tool for controlling WDE and the risks associated with those emissions, it seems logical that research is urgently required to determine the potential applicability of MICP-driven biocementation in tailing deposits.

This study aimed to evaluate the capacity of the MICP process to induce changes in tailing mechanical properties. For this purpose, the effect of different doses of biocemented reagents was evaluated, and two different methods for adding biocement reagents were compared.

## 2. Materials and Methods

### 2.1. Microorganism and Cultivation Conditions

This research was conducted using the microorganism *Sporosarcina pasteurii* NCIMB 8841. Biomass required for biocementation assays was produced by cultivation under batch conditions at 30 °C and 120 rpm.

Biomass concentration was estimated by measuring optical density, determined by spectrophotometry, at a wavelength of 600 nm. The relation between optical density and cell concentration (determined by dry cellular weight) was established by a calibration curve. Cell count was also determined by microscopic observation using a Neubauer counting chamber. Relation between cells concentration and cell count was established according to the following equation:

$$[Cell]_{conc} = 1.82 \times 10^{-7} [Cell]_{count} - 0.88 \quad (1)$$

where  $[cell]_{conc}$  is the value of cell concentration expressed in  $g L^{-1}$  and  $[cell]_{count}$  is the cell count expressed in cells  $mL^{-1}$ .

The composition of the culture medium was 1  $g L^{-1}$  nutrient broth, 2  $g L^{-1}$  yeast extract, 5  $g L^{-1}$  peptone and 5  $g L^{-1}$  NaCl and 20  $g L^{-1}$  urea [37]. Culture medium without urea was sterilized in an autoclave at 121 °C for 30 min. Urea solution was sterilized using a 0.22  $\mu m$  sterile filtration system to prevent thermal decomposition.

### 2.2. Biocementation Assays

A series of biocementation assays were conducted to determine the capacity of MICP to induce changes in tailing mechanical properties. Two testing materials were used. The first was natural sand, conceived as a control to facilitate comparison with results available in the literature. The second was a synthetic tailing, prepared from selected soil materials according to Gorakhki and Bareither [38,39]. Synthetic tailing was subjected to sieving in order to provide a particle size distribution (PSD) similar to that of natural mine tailings [12,40]. Soil materials were obtained from an aggregate processing company located in the region of Valparaíso, Chile. Geotechnical characterization of sand and synthetic tailing sample included mechanical sieve (ASTM D422-63, [41]), pH (ASTM D4972-19, [42]), specific gravity (ASTM D854-14, [43]), and hydraulic conductivity (ASTM D2434-22, [44]). A summary of the geotechnical characterization of the sand and synthetic tailing is presented in Table 1. Before assays were conducted, samples were dried in an oven at 65 °C for 24 h.

**Table 1.** Geotechnical characteristics of sand and synthetic tailing used for biocemented assays.

Parameter		Sample	
Type of soil	Particle size ( $\mu m$ )	Synthetic tailing	Sand
Medium sand	>250	67.4%	85.6%
Fine sand	250–106	30.2%	12%
Loamy fine sand	106–75	1.5%	1.7%
Silt	<75	0.9%	0.7%
	pH	7.8	8.5
	Specific gravity	2.5 ( $g mL^{-1}$ )	1.9 ( $g mL^{-1}$ )
	Minimum dry density	1.9 ( $g mL^{-1}$ )	1.5 ( $g mL^{-1}$ )
	Hydraulic conductivity	$7.21 \times 10^{-5}$ ( $cm s^{-1}$ )	$10^{-4}$ ( $cm s^{-1}$ )

Biocementation assays were conducted using polyurethane cups as molds, according to the procedure described by Hamdan et al. [40]. The polyurethane molds had a diameter of 5 cm and a total volume of 100 mL. First, 30 g of the material was placed in the molds, and then biomass suspension and biocementation media were added. Biocementation media consisted of a solution of urea and  $CaCl_2$ . Then, samples were left to cure and dry at 30 °C for 10 days. Each tested condition was replicated four times. In all experiments, the combined volumes of bacterial suspension and biocementation media were kept constant at 0.33 L per  $kg_{drysoil}$  (equivalent to 5 L per  $m^2$  of surface treated). Different doses of calcium

were added in different experiments by changing the concentration of  $\text{CaCl}_2$  and urea, always keeping their molar ratio constant at 3:1.

Table 2 presents a summary of the biocementation assays performed during this research. Assays 1 and 2 were performed by adding  $\text{CaCl}_2$  in the range 0–1.1 M to evaluate the effect of MICP on sand and synthetic tailing samples. Biocementation media was added using irrigation method, which consisted of adding the media on top of the testing cup, enabling the solution to permeate through the sample (i.e., testing cup was perforated in the bottom). During assay 3, conditions were kept constant, but biocementation media was added using the mixing method. In this case, the tailing sample was mixed with biocementation media in the testing cup, using a vortex shaker to homogenize and remove trapped air. During mixing method, the media was contained, i.e., testing cups were not perforated at the bottom. Finally, assay 4 tested a larger calcium concentration range (0–2.5 M). All assays in Table 2 involved the same biomass dosage (0.06 g per  $\text{kg}_{\text{drysoil}}$ ) and the same urea:calcium molar ratio (3:1).

**Table 2.** Description of biocementation assays.

Assay	Soil Sample	Addition of Biocementation Media	Biomass ( $\text{g L}^{-1}$ )	$\text{CaCl}_2$ (M)	Biomass Dose ( $\text{g kg}^{-1}_{\text{drysoil}}$ )	$\text{CaCl}_2$ Dose ( $\text{mol kg}^{-1}_{\text{drysoil}}$ )
1	Sand	Irrigation	0.90	0, 0.3, 1.1	0.06	0, 0.2, 0.7
2	Synthetic tailing	Irrigation	0.90	0, 0.3, 1.1	0.06	0, 0.2, 0.7
3	Synthetic tailing	Mixing	0.90	0, 0.3, 1.1	0.06	0, 0.2, 0.7
4	Synthetic tailing	Mixing	0.90	0–2.5	0.06	0–1.5

Observation: Biomass and  $\text{CaCl}_2$  concentrations indicated refer to the amount of water added to each assay (0.33 L per  $\text{kg}_{\text{drysoil}}$ ).

Results are expressed as mean  $\pm$  standard deviation. Existence of statistical differences was verified by Student's *t*-test and analysis of variance using the MINITAB software [45]. Observed differences were considered statistically significant at *p*-values < 0.05.

### 2.3. Analytic Methods

#### 2.3.1. Biocementation Effect

Different methodologies have been proposed to assess the capacity of MICP to increase bearing capacities of soil, such as unconfined compression tests, shear strength tests, penetration cone tests and thermal conductivity measurements [31,46–48]. In this work, the cone penetration test and thermal conductivity were selected to evaluate the performance of the MICP treatment.

Cone penetration test was used to measure the surface strength of the biocemented samples. High values could be then related with an increased resistance to wind erosion. Cone penetration test was performed with an electric compression press (ELE international, mod. T-1325A-4). The penetration cone was adjusted above the surface of biocemented sample before starting the test. Then, penetration cone with a flat-ended surface was set to penetrate 10 mm into the sample at a rate of  $1.0 \text{ mm min}^{-1}$ . The surface of the cone varied from 0.5 to  $2.5 \text{ cm}^2$ , depending on the strength of the sample [27].

Thermal conductivity is expected to respond to different levels of biocementation due to the formation of  $\text{CaCO}_3$  bridges between the particles [48,49]. Thermal conductivity was determined using an SH-3 dual sensor (Thermal properties analyzer, Tempos). The length of the thermocouples was 30 mm with a diameter of 1.2 mm and 6 mm spacing. Due to the high strength of biocemented samples, two holes with the dimensions of the thermocouples were drilled horizontally in the biocemented samples, where the SH-3 sensor was inserted.

#### 2.3.2. Ureolytic Activity

Ureolytic activity was determined by measuring the amount of ammonia released by the hydrolysis of urea using the phenol-hypochlorite test method [37,50]. One unit of

enzymatic activity (U) is defined as the amount of urease that hydrolyses 1  $\mu\text{mol}$  urea per minute.

### 2.3.3. $\text{CaCO}_3$ Content of the Biocemented Sample

Representative samples were taken from biocemented material, which was dried for 24 h at 105 °C. Then, 1 g of dried material was washed with 25 mL of distilled water and centrifuged at 10,000 rpm for 5 min. Supernatant containing unreacted soluble calcium was discharged. To remove interference coming from organic matter, sample was subjected to calcination for 5 h at 550 °C [51]. Calcined sample was then washed with 10 mL of 2 M HCl solution and left to react for 6 h. Sample pH was adjusted to 7.0 and then filtered using an MN 616 paper filter to remove solids. Filtrate was recovered and titrated with EDTA to determine the calcium concentration [51].

### 2.3.4. Micrographical and Mineralogical Analysis

The micrographical features of the precipitated crystals were observed by scanning electron microscopy (SEM) using HITACHI SU3500 equipment at accelerating voltages of 10 kV and WD 6 mm. Secondary electron imaging (SEI) and backscattered electron imaging (BSEI) techniques were used for electron micrography.

FTIR analysis was used to identify the mineralogical features of the precipitated crystals. The spectra were acquired by a JASCO FT/IR-4600 spectrometer, using a diamond single reflection attenuated total reflectance (FTIR-ATR). Spectra were obtained with 64 scans per spectrum, at a spectral resolution of 0.5  $\text{cm}^{-1}$ , in the range of 4000 to 600  $\text{cm}^{-1}$ . Baseline correction and scaling normalization were made in Wiley's KnowItAll™ Software. Spectral analysis was made to promote a better understanding of the peaks position and intensity. Deconvolution was made using Origin 2019 PRO software by modeling the spectra to a Gaussian function (Equation (2)).

$$y = y_0 + \frac{A e^{-\frac{4 \ln(2)(X-X_C)^2}{W^2}}}{W \sqrt{\frac{\pi}{4 \ln(2)}}} \quad (2)$$

where  $y$  is the intensity of the peak at a wavenumber  $X$ ,  $y_0$  is the base intensity,  $X_C$  is the center of the peak ( $\text{cm}^{-1}$ ),  $A$  is the area and  $W$  is full width at half maximum (FWHM).

Quantitative X-ray diffraction (XRD) analysis was used to determine the nature of the precipitated calcium. The XRD patterns were collected by scanning between 10° and 90° ( $2\theta$ ) in the continuous mode by employing a Bruker D8 Advance Diffractometer, using Cu  $K\alpha$  ( $k = 1.54 \text{ \AA}$ ) radiation. The diffractometer was run in the continuous mode with an integrated step scan of 0.020° ( $2\theta$ ), using a PIXcel detector with a time per step of 340 s. To quantitatively examine the polymorph content of  $\text{CaCO}_3$  precipitates, the sample XRD patterns were analyzed using the Rietveld refinement method [52] with the material analysis using a diffraction package.

Before micrographical and mineralogical analysis, 1–2 g of samples were passed through a sieve (Mesh N° 50) to remove fine particles, favoring the presence of particles containing precipitated  $\text{CaCO}_3$  to facilitate the analyses.

## 3. Results and Discussion

### 3.1. Assays to Characterize the MICP Precipitation Process

Biomass suspension used for biocementation assays was applied at a concentration of  $0.90 \pm 0.01 \text{ g L}^{-1}$ , equivalent to  $5.0 \pm 0.1 \times 10^6 \text{ cells mL}^{-1}$ . Ureolytic activity was  $78.3 \pm 6.8 \text{ U mL}^{-1}$ . Thermal conductivity, surface strength,  $\text{CaCO}_3$  content and calcium precipitation yield during assays 1 and 2 are shown in Figure 1. Precipitation yield refers to the proportion of added calcium found in the form of calcium carbonate due to the bioprecipitation phenomenon. Results show that application of different levels of  $\text{CaCl}_2$  induced little or no changes in thermal conductivity (Figure 1A). Biocemented sand and

tailing showed similar thermal conductivities of about  $0.20 \text{ W m}^{-2} \text{ K}^{-1}$ . On the other hand, results show a relevant increase in surface strength (Figure 1B) when applying increasing levels of  $\text{CaCl}_2$ . Biocemented samples treated with 1.1 M  $\text{CaCl}_2$  presented an average strength of 1000–1500 kPa, three times higher than those without calcium addition (Figure 1B). The surface strength achieved in this study is higher than that observed in other studies on soil biocementation using *S. pasteurii* under similar conditions. Katebi et al. [53] reported a penetration strength of 250 kPa when applying MICP to sand samples using a similar dosage of biocementation media ( $0.3 \text{ L kg}^{-1} \text{ drysoil}$ ). On the other hand, Meng et al. [20] reported that biocemented sand achieved a surface strength of about 366 kPa. The difference may be related to using the equimolar urea:calcium ratio.

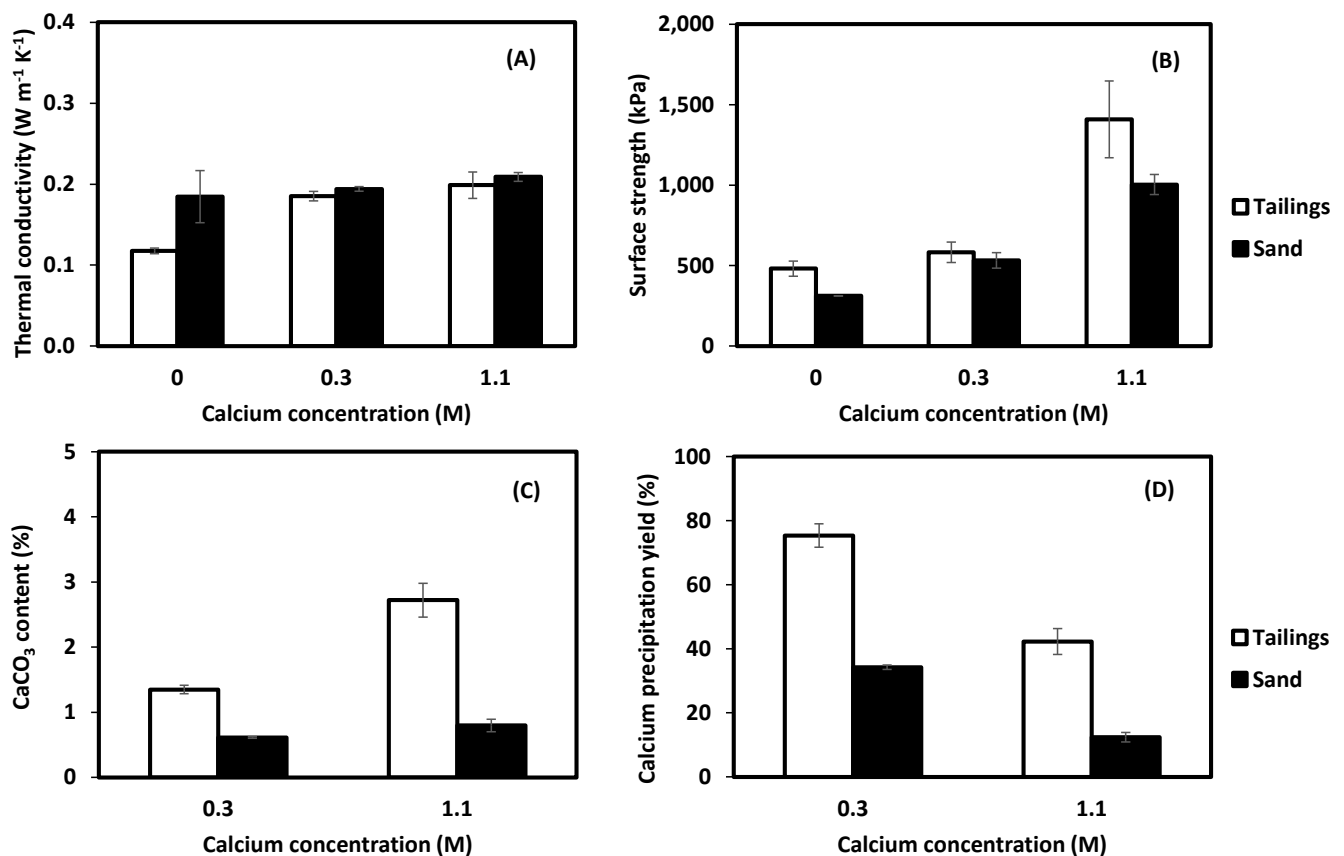


**Figure 1.** Performance of MICP applied for the biocementation of sand and synthetic tailings. (A) Thermal conductivity, (B) surface strength determined by cone penetration method, (C)  $\text{CaCO}_3$  content, (D) calcium precipitation yield. Error bars represent the standard deviation between quadruplicates.

Figure 1C,D shows that precipitation occurred at a greater extent in the tailing. Differences between tailing and sand were statistically significant ( $p$ -value < 0.05). In the case of tailing,  $\text{CaCO}_3$  content, and precipitation yield were close to 3% and 40%, respectively, when 1.1 M of  $\text{CaCl}_2$  was applied. This may result from a lower hydraulic conductivity of tailings, with respect to sand (2.5 times lower), which increases retention of biocementation media, providing a longer reaction time and favoring precipitation [26]. Our results are in agreement with those of Lai et al. [23], who also observed higher levels of biocementation on iron tailing than in quartz sand. Therefore, the results shown in Figure 1 suggest that tailings may indeed provide an environment enabling effective MICP driven by *S. pasteurii*.

As depicted in Table 2, assay 3 was performed under the same conditions as 2 but with a different supply method for the biocementation media. A comparison of the performance of both methods (assays 2 and 3) is presented in Figure 2 for tailings. Results show an increase in thermal conductivity as  $\text{CaCl}_2$  concentration was progressively increased from 0.3 to 1.1 M. Results also show a dramatic increase in surface strength when the mixing

method was applied. The results show that the method of supplying the biocementation medium and the concentration of  $\text{CaCl}_2$  applied were statistically significant factors ( $p$ -value 0.001) when thermal conductivity and surface strength were considered responses. Figure 2 indicates that using mixing methods with a  $\text{CaCl}_2$  concentration of 1.1 M induced thermal conductivity ( $0.26 \pm 0.02 \text{ W m}^{-2} \text{ K}^{-1}$ ) and surface strength ( $7432 \pm 932 \text{ kPa}$ ), 2 and 5 times higher than the assays without calcium addition. Moreover, the maximum  $\text{CaCO}_3$  content was almost 6%, similar to that reported by Wang et al. [49].

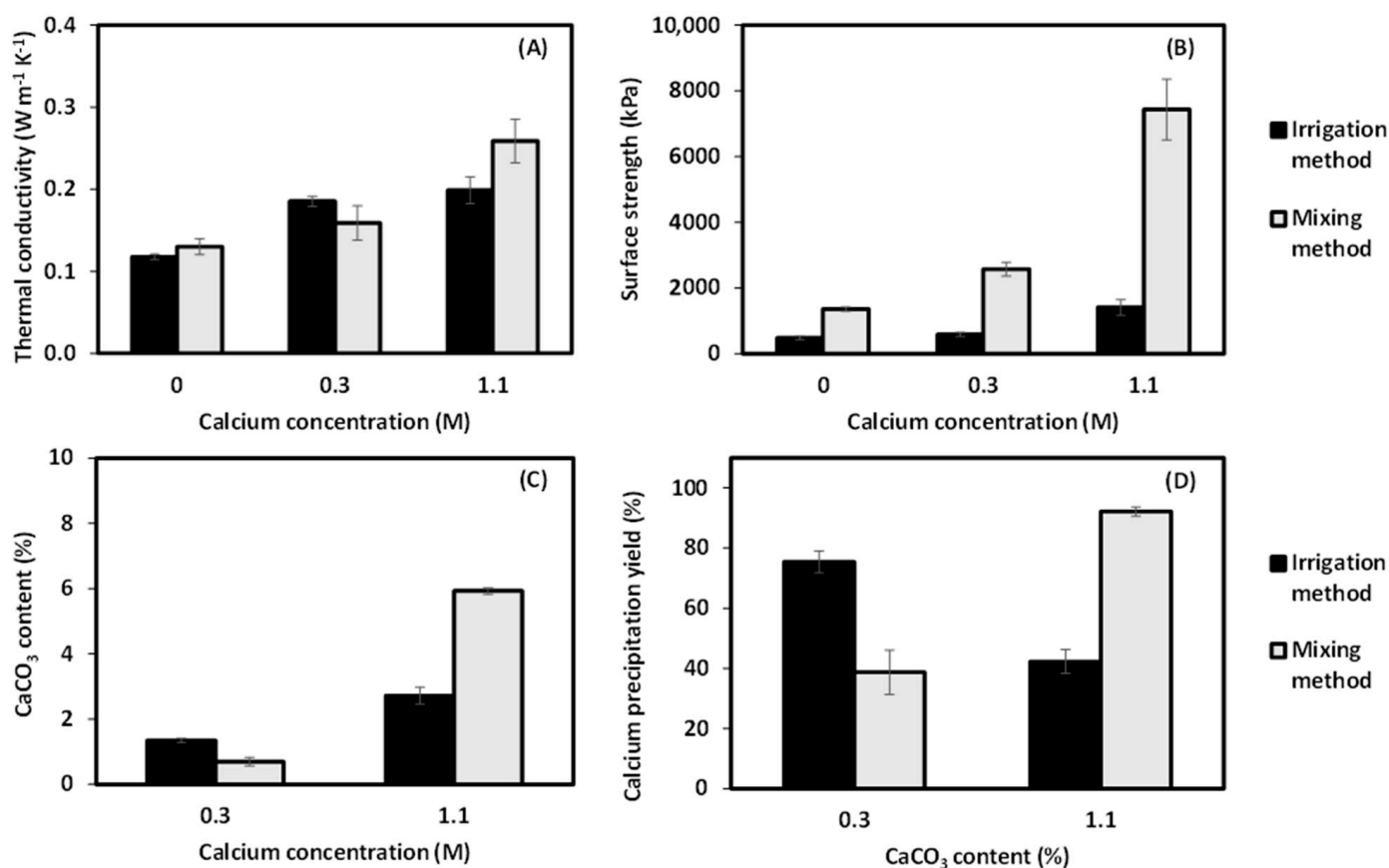


**Figure 2.** Performance of MICP process applied for the biocementation of synthetic tailing, using irrigation and mixing methods for the addition of biocementation medium. (A) Thermal conductivity, (B) surface strength by cone penetration method, (C)  $\text{CaCO}_3$  content, (D) calcium precipitation yield. Error bars represent the standard deviation between quadruplicates.

Moreover, at a  $\text{CaCl}_2$  concentration of 1.1 M, the mixing method provided twice the  $\text{CaCO}_3$  content and calcium precipitation yield than the irrigation method. Again, the reason can be ascribed to the low hydraulic conductivity of tailings ( $7.21 \times 10^{-5} \text{ cm s}^{-1}$ ), which limited the permeation and distribution of the biocementation medium. Then, the substantial biocementation improvement induced by the mixing method can be attributed to the mechanical mixing, which promotes a more homogeneous  $\text{CaCO}_3$  precipitation, enhancing the bearing effect induced by MICP. Our results are in agreement with those of Chae et al. [26], who also observed that calcite precipitated uniformly in the fine sand when the mixing method was applied.

Previous results identified a clear relation between  $\text{CaCO}_3$  content and surface strength. In order to clarify if such a relation remains when providing a more intensive treatment, assay 4 was performed, using  $\text{CaCl}_2$  concentration in the range 0–2.5 M. Biomass dosage and urea:calcium molar ratio was kept at the same values used in previous assays. Figure 3A,B shows that the surface strength and  $\text{CaCO}_3$  content increase when the  $\text{CaCl}_2$  concentration is increased, which is in agreement with Meng et al. [20]. A maximum surface strength of

12,241 ± 1670 kPa was reached (at 1.8 M of CaCl<sub>2</sub>), a value higher than those reported by other studies under similar conditions [21,27]. For example, Ehsasi et al. [27] reported a surface strength of 4990 kPa, and a CaCO<sub>3</sub> content of 3% (in a crust layer). Differences may be related to using a lower calcium dose, different urea:calcium ratio, tailing composition and/or particle size. Figure 3C suggests the presence of a maximum in the calcium precipitation yield (a little over 90%) at 1.1 M of CaCl<sub>2</sub> concentration. As a result, further increases in CaCl<sub>2</sub> resulted in a decrease in yield, which may be a consequence of the inhibition of ureolysis by high Ca<sup>2+</sup> concentrations [54]. Unhydrolyzed urea may re-consolidate as a crystal as the tailing dries, which does not contribute to mechanical strength and may even reduce it. To analyze this effect, the CaCO<sub>3</sub> content and its relationship with surface strength is illustrated in Figure 3D. This figure shows the existence of a maximum over which a decrease in surface strength exists. This behavior may be indeed related to the re-consolidation of unconverted urea. Then, according to Figure 3, it would not be possible to provide higher levels of biocementation by simply increasing the dosage of calcium or urea.

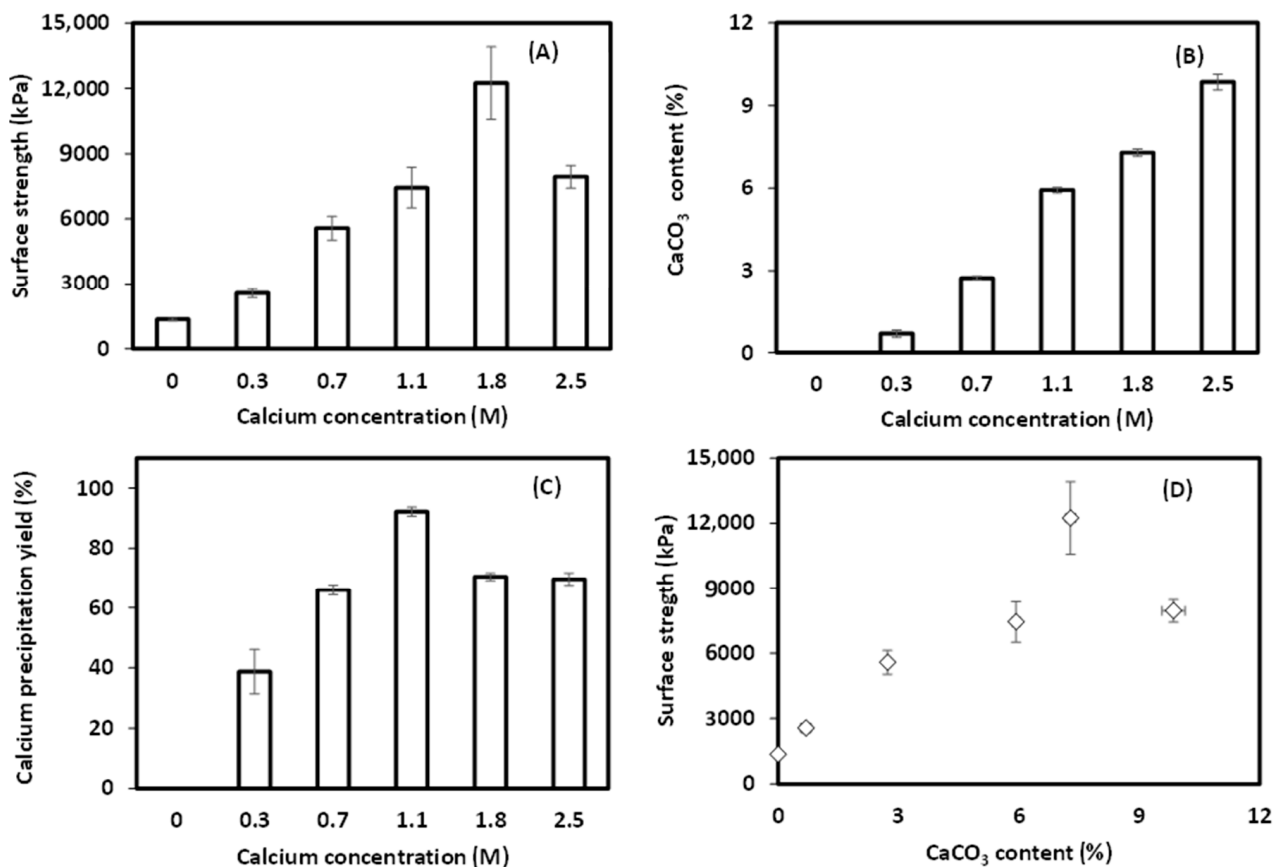


**Figure 3.** Performance of MICP applied for the biocementation of synthetic tailing, using mixing methods for the addition of biocementation medium. (A) Surface strength by cone penetration method, (B) CaCO<sub>3</sub> content, (C) calcium precipitation yield, (D) relationship between surface strength and CaCO<sub>3</sub> content. Error bars represent the standard deviation between quadruplicates.

### 3.2. Micrographical and Mineralogical Analysis of Synthetic Tailing Samples Treated by MICP

The surface microstructure of tailings was observed by SEM analysis. Figure 4 presents SEM images of untreated tailing (Figure 4A) and biocemented tailing using the mixing method at a concentration of 1.1 M of CaCl<sub>2</sub> (Figure 4B). SEM images show the dramatic effect that biocementation treatment induced. No bonding patterns were identified in the untreated sample. Instead, the image shows individual particles, loosely stacked and with smooth surfaces (indicated by yellow circles in Figure 4A).

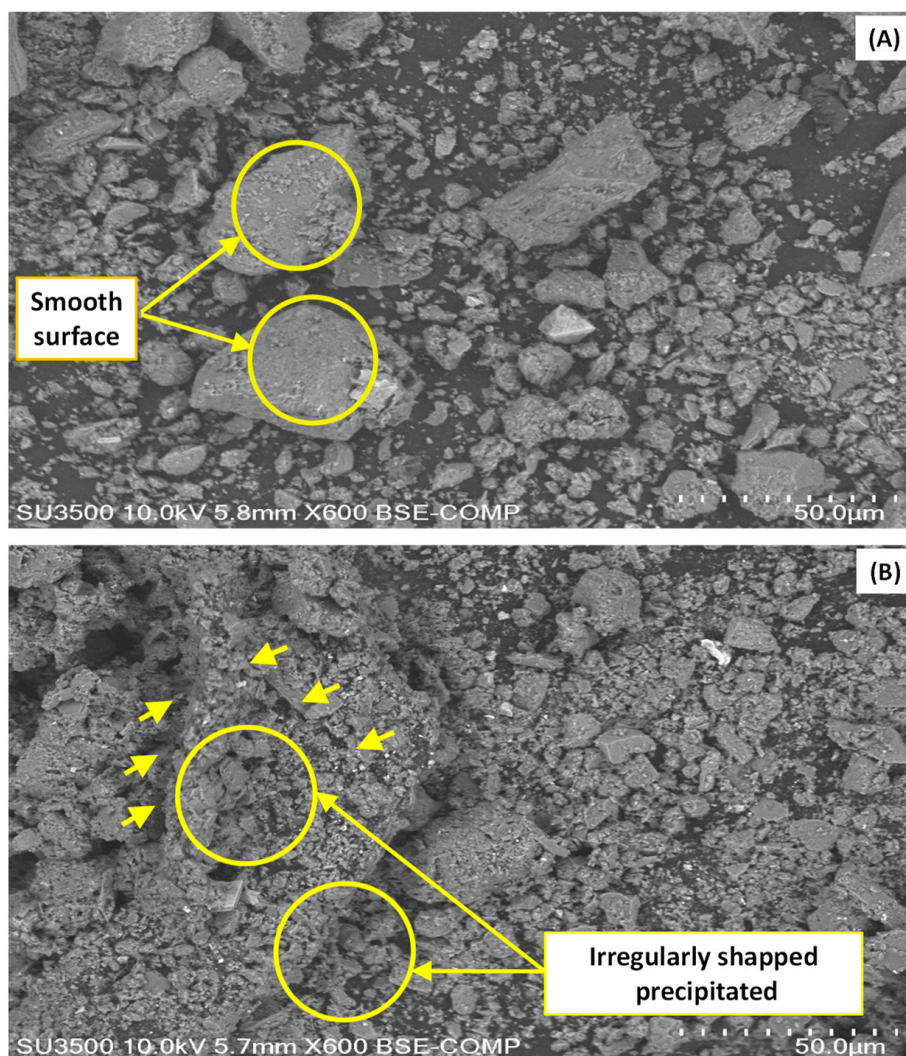


**Figure 4.** SEM micrographs of (A) untreated tailing sample and (B) biocemented tailing sample treated by mixing method at 1.1 M  $\text{CaCl}_2$ . In image (B), yellow circles indicate the presence of irregularly shaped precipitates on biocemented tailing particles. Yellow arrows indicate the presence of binding patterns between biocemented tailing particles (image (B)).

On the other hand, Figure 4B shows that biocemented samples presented irregularly shaped precipitates, that were relatively sparse, with some of them deposited on the surface of the tailing particles (indicated by yellow circles in Figure 4B). In addition, it can be observed that the biocemented sample has bonding patterns due to a large number of irregularly shaped precipitates between the tailing particles, presumably acting as bridges (indicated by yellow arrows in Figure 4B). This observation is similar to Bu et al. [55] and Duo et al. [29]. Furthermore, this phenomenon correlates well with the observed improved surface strength (see Figure 3A) and is consistent with previous studies [32,56,57].

Mineralogical features of the precipitated crystals were identified by FTIR analysis. Figure 5A presents the FTIR spectra of untreated tailing, and Figure 5B shows the spectra of the biocemented tailing using the mixing method at a concentration of 1.1 M of  $\text{CaCl}_2$ . Peaks in the range  $3000\text{ cm}^{-1}$  and  $3600\text{ cm}^{-1}$  were observed in the case of the biocemented sample (Figure 5B), which correlate with the stretching of O-H and N-H bonds [58], suggesting the presence of unhydrolyzed urea. This is supported by the differences observed in the peaks at  $1590\text{ cm}^{-1}$ ,  $1615\text{ cm}^{-1}$  and  $1660\text{ cm}^{-1}$ , which are correlated with the  $\nu(\text{CO})$ ,  $\delta_s(\text{NH}_2)$  and  $\delta_s(\text{NH}_2)$  vibrations of urea [59,60].

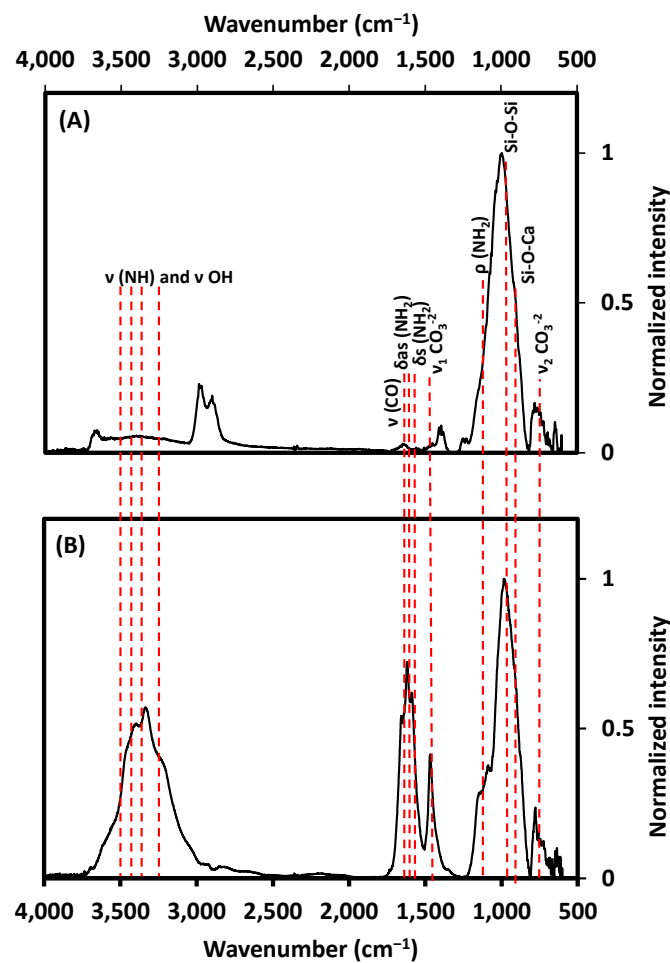


**Figure 5.** IR spectra of (A) Untreated sample, (B) Biocemented sample treated by mixing method at 1.1 M of  $\text{CaCl}_2$ . Detail of the symbology:  $\nu$ : stretching,  $\delta_{as}$ : asymmetric bending,  $\delta_s$ : symmetric bending  $\rho$ : in-plane bending (rocking).  $\nu_1 \text{CO}_3^{-2}$  is the asymmetric stretching of the carbonate.  $\nu_2 \text{CO}_3^{-2}$  is the in-plane bending of the carbonate.

To assess with better precision the IR spectra changes in the range between  $1200 \text{ cm}^{-1}$  and  $800 \text{ cm}^{-1}$ , a deconvolution of the spectra was made according to Equation (3). An increase in the peak at  $913 \text{ cm}^{-1}$  was observed (Figure 5B), which can be attributed to Si-O-Ca bonds [61,62], indicating a possible chemical interaction between the synthetic tailing and calcium ion, which may have induced some bearing effect on the tailing particles. Chemical interaction between Ca and Si may occur when traces of calcium remain unprecipitated. This could happen because of a deficit of inorganic carbon available due to an inhibition of the urease enzyme at high calcium concentrations [54]. This may explain the presence of a fraction of unhydrolyzed urea, as identified above. Spectra also shows a peak at  $1468 \text{ cm}^{-1}$ , which may be attributed to the asymmetric stretching of the carbonate ion [62–65]. Additionally, the peak at  $780 \text{ cm}^{-1}$  may be correlated with the in-plane bending of the carbonate (Figure 5B), indicating that  $\text{CaCO}_3$  was present in a crystalline form, presumably vaterite or calcite [52]. This may explain the observed irregularly shaped precipitates (see Figure 4B) and the improved surface strength (see Figure 3A).

XRD analysis was used to identify the type of crystals formed during biocementation. Table 3 shows the detail of the crystalline phases of untreated and biocement tailings (by the mixing method). Several general observations can be derived from the presented data. Probably the most relevant is that precipitated calcium exists as anorthite and  $\text{CaCO}_3$ , the first in the predominant form. Anorthite is a porous ceramic that occurs naturally on the earth's surface and is composed of calcium oxide, corundum and silica [66]. It was

not present in the untreated tailing, so it was inferred that it was produced during MICP treatment due to the chemical interaction between Ca and Si [61]. Vaterite and calcite were the crystalline forms of  $\text{CaCO}_3$  that were mainly produced, which is consistent with previous studies [23,34]. Table 3 also shows that the application of treatment using 1.1 M of  $\text{CaCl}_2$  induced a higher concentration of anorthite, vaterite and calcite compared to the other treatments, which correlates well with the significant improvement of surface strength (Figure 3A).

**Table 3.** Detail the crystalline phases of untreated and biocemented tailing treated by the mixing method at different calcium concentrations.

Type of Treatment	$\text{CaCl}_2$ (M)	Composition (%)						
		Albite	Quartz	Sanidine	Kaolinite	Anorthite	Vaterite	Calcite
Untreated	-	67.2	23.9	6.9	2	0	0	0
MICP	0.3	30.3	13.9	24.6	0	31.1	0.2	0
	1.1	5.4	24.4	6.5	0	51.4	8	4.2
	2.5	30.1	16.9	17.7	0	33	1.3	1.1

It should be noted that the results derived from micrographic and mineralogical characterization (SEM, FTIR and XRD analysis) showed good consistency and helped to identify the mechanisms through which MICP successfully increased the mechanical strength of tailing. The results of this study demonstrate that tailing provides a suitable environment for the successful application of MICP as a bearing agent to produce a precipitated  $\text{CaCO}_3$  surface crust on tailing material.

#### 4. Conclusions

- Tailings offer a promising environment for the application of MICP. Biocemented tailings showed a relevant improvement in their mechanical surface strength, which may imply a potential use to control wind-blown dust emissions from tailing deposits.
- $\text{CaCl}_2$  dosage represents an important factor governing the ability of MICP to induce a bearing capacity on tailings. Therefore, an increase in calcium dosage should induce increments in surface strength. However, a maximum was detected, over which further increases in  $\text{CaCl}_2$  dosage produce no improvements in the treatment.
- The method for reagent supplementation is also a key factor in determining the biocementation of tailings. The use of mechanical mixing of biocementation reagents and tailings induces a more homogeneous treatment that substantially improves the surface strength of the biocemented material.
- Micrographical and mineralogical analysis showed how MICP treatment increases the bonding patterns between tailings particles through the formation of bridges by calcium precipitates present in the form of an anorthite-calcite-vaterite crystalline form. In addition, chemical interaction between tailings and calcium ions in the crystalline form of anorthite was observed, a phenomenon that has not been reported before.

**Author Contributions:** Conceptualization, H.Z.-B., E.O.-M. and D.J.; methodology, H.Z.-B. and E.O.-M.; formal analysis, H.Z.-B., E.O.-M. and D.J.; investigation, H.Z.-B.; resources, D.J., M.R. and L.J.; writing—original draft preparation, H.Z.-B., E.O.-M. and D.J.; writing—review and editing, D.J., H.Z.-B., J.T.-A., L.J., Á.T.-A. and M.R.; supervision, D.J., M.R., E.O.-M. and J.T.-A.; project administration, D.J. and M.R.; funding acquisition, D.J. and M.R. All authors have read and agreed to the published version of the manuscript.

**Funding:** This research was funded by ANID through project ANID/FONDECYT/1190664. Héctor Zúñiga acknowledges the support provided by the ANID doctorate scholarship N° 21201013.

**Institutional Review Board Statement:** Not applicable.

**Informed Consent Statement:** Not applicable.

**Data Availability Statement:** Not applicable.

**Acknowledgments:** Authors wish to acknowledge the support provided by the CRHIAM center (ANID/FONDAP/15130015).

**Conflicts of Interest:** The authors declare no conflict of interest.

## References

1. Carvalho, F.P. Mining Industry and Sustainable Development: Time for Change. *Food Energy Secur.* **2017**, *6*, 61–77. [[CrossRef](#)]
2. Pedro, A.; Ayuk, E.T.; Bodourogrou, C.; Milligan, B.; Ekins, P.; Oberle, B. Towards a Sustainable Development Licence to Operate for the Extractive Sector. *Miner. Econ.* **2017**, *30*, 153–165. [[CrossRef](#)]
3. Kossoff, D.; Dubbin, W.E.; Alfredsson, M.; Edwards, S.J.; Macklin, M.G.; Hudson-Edwards, K.A. Mine Tailings Dams: Characteristics, Failure, Environmental Impacts, and Remediation. *Appl. Geochem.* **2014**, *51*, 229–245. [[CrossRef](#)]
4. Buikema, N.D.; Zwissler, B.E.; Seagren, E.A.; Oommen, T.; Vitton, S. Stabilisation of Iron Mine Tailings through Biocalcification. *Environ. Geotech.* **2017**, *5*, 94–106. [[CrossRef](#)]
5. Meng, H.; Shu, S.; Gao, Y.; He, J.; Wan, Y. Kitchen Waste for *Sporosarcina Pasteurii* Cultivation and Its Application in Wind Erosion Control of Desert Soil via Microbially Induced Carbonate Precipitation. *Acta Geotech.* **2021**, *16*, 4045–4059. [[CrossRef](#)]
6. Csavina, J.; Field, J.; Taylor, M.P.; Gao, S.; Landázuri, A.; Betterton, E.A.; Sáez, A.E. A Review on the Importance of Metals and Metalloids in Atmospheric Dust and Aerosol from Mining Operations. *Sci. Total Environ.* **2012**, *433*, 58–73. [[CrossRef](#)]
7. Jaishankar, M.; Tseten, T.; Anbalagan, N.; Mathew, B.B.; Beeregowda, K.N. Toxicity, Mechanism and Health Effects of Some Heavy Metals. *Interdiscip. Toxicol.* **2014**, *7*, 60–72. [[CrossRef](#)]
8. Gil-Loaiza, J.; White, S.A.; Root, R.A.; Solís-Dominguez, F.A.; Hammond, C.M.; Chorover, J.; Maier, R.M. Phytostabilization of Mine Tailings Using Compost-Assisted Direct Planting: Translating Greenhouse Results to the Field. *Sci. Total Environ.* **2016**, *565*, 451–461. [[CrossRef](#)]
9. Park, J.; Kim, K.; Lee, T.; Kim, M. Tailings Storage Facilities (TSFs) Dust Control Using Biocompatible Polymers. *Min. Metall. Explor.* **2019**, *36*, 785–795. [[CrossRef](#)]
10. Solís-Dominguez, F.A.; White, S.A.; Hutter, T.B.; Amistadi, M.K.; Root, R.A.; Chorover, J.; Maier, R.M. Response of Key Soil Parameters during Compost-Assisted Phytostabilization in Extremely Acidic Tailings: Effect of Plant Species. *Environ. Sci. Technol.* **2012**, *46*, 1019–1027. [[CrossRef](#)]
11. Almajed, A.; Lateef, M.A.; Moghal, A.A.B.; Lemboye, K. State-of-the-Art Review of the Applicability and Challenges of Microbial-Induced Calcite Precipitation (MICP) and Enzyme-Induced Calcite Precipitation (EICP) Techniques for Geotechnical and Geoenvironmental Applications. *Crystals* **2021**, *11*, 370. [[CrossRef](#)]
12. Chen, R.; Lee, I.; Zhang, L. Biopolymer Stabilization of Mine Tailings for Dust Control. *J. Geotech. Geoenviron. Eng.* **2015**, *141*, 04014100. [[CrossRef](#)]
13. Yuge, K.; Anan, M. Evaluation of the Effect of Wind Velocity and Soil Moisture Condition on Soil Erosion in Andosol Agricultural Fields (Model Experiment). *Water* **2019**, *11*, 98. [[CrossRef](#)]
14. Dejong, J.T.; Soga, K.; Kavazanjian, E.; Burns, S.; Van Paassen, L.A.; Al Qabany, A.; Aydilek, A.; Bang, S.S.; Burbank, M.; Caslake, L.F.; et al. Biogeochemical Processes and Geotechnical Applications: Progress, Opportunities and Challenges. *Geotechnique* **2013**, *63*, 287–301. [[CrossRef](#)]
15. Dejong, J.T.; Mortensen, B.M.; Martinez, B.C.; Nelson, D.C. Bio-Mediated Soil Improvement. *Ecol. Eng.* **2010**, *36*, 197–210. [[CrossRef](#)]
16. Rahman, M.M.; Hora, R.N.; Ahenkorah, I.; Beecham, S.; Karim, M.R.; Iqbal, A. State-of-the-Art Review of Microbial-Induced Calcite Precipitation and Its Sustainability in Engineering Applications. *Sustain* **2020**, *12*, 6281. [[CrossRef](#)]
17. Song, M.; Ju, T.; Meng, Y.; Han, S.; Lin, L.; Jiang, J. A Review on the Applications of Microbially Induced Calcium Carbonate Precipitation in Solid Waste Treatment and Soil Remediation. *Chemosphere* **2022**, *290*, 133229. [[CrossRef](#)]
18. Zúñiga-Barra, H.; Toledo-Alarcón, J.; Torres-Aravena, Á.; Jorquera, L.; Rivas, M.; Gutiérrez, L.; Jeison, D. Improving the Sustainable Management of Mining Tailings through Microbially Induced Calcite Precipitation: A Review. *Miner. Eng.* **2022**, *189*, 107855. [[CrossRef](#)]
19. Achal, V.; Mukherjee, A.; Kumari, D.; Zhang, Q. Biomineralization for Sustainable Construction—A Review of Processes and Applications. *Earth Sci. Rev.* **2015**, *148*, 1–17. [[CrossRef](#)]
20. Meng, H.; Gao, Y.; He, J.; Qi, Y.; Hang, L. Microbially Induced Carbonate Precipitation for Wind Erosion Control of Desert Soil: Field-Scale Tests. *Geoderma* **2021**, *383*, 114723. [[CrossRef](#)]
21. Omoregie, A.I.; Palombo, E.A.; Ong, D.E.L.; Nissom, P.M. Biocementation of Sand by *Sporosarcina Pasteurii* Strain and Technical-Grade Cementation Reagents through Surface Percolation Treatment Method. *Constr. Build. Mater.* **2019**, *228*, 116828. [[CrossRef](#)]
22. Whiffin, V.S.; van Paassen, L.A.; Harkes, M.P. Microbial Carbonate Precipitation as a Soil Improvement Technique. *Geomicrobiol. J.* **2007**, *24*, 417–423. [[CrossRef](#)]
23. Lai, Y.; Yu, J.; Liu, S.; Liu, J.; Wang, R.; Dong, B. Experimental Study to Improve the Mechanical Properties of Iron Tailings Sand by Using MICP at Low PH. *Constr. Build. Mater.* **2021**, *273*, 121729. [[CrossRef](#)]
24. Tian, K.; Wu, Y.; Zhang, H.; Li, D.; Nie, K.; Zhang, S. Increasing Wind Erosion Resistance of Aeolian Sandy Soil by Microbially Induced Calcium Carbonate Precipitation. *Land Degrad. Dev.* **2018**, *29*, 4271–4281. [[CrossRef](#)]

25. Zhang, Z.J.; Li, B.; Hu, L.; Zheng, H.M.; He, G.C.; Yu, Q.; Wu, L.L. Experimental Study on MICP Technology for Strengthening Tail Sand under a Seepage Field. *Geofluids* **2020**, *2020*, 8819326. [[CrossRef](#)]
26. Chae, S.H.; Chung, H.; Nam, K. Evaluation of Microbially Induced Calcite Precipitation (MICP) Methods on Different Soil Types for Wind Erosion Control. *Environ. Eng. Res.* **2021**, *26*, 190507. [[CrossRef](#)]
27. Ehsasi, F.; van Paassen, L.; Wang, L. Stabilization of Mine Tailings Using Microbiological Induced Carbonate Precipitation for Dust Mitigation: Treatment Optimization and Durability Assessment. *Geo Congr.* **2022**, *2022*, 326–334.
28. Meyer, F.D.; Bang, S.; Min, S.; Stetler, L.D.; Bang, S.S. Microbiologically-Induced Soil Stabilization: Application of *Sporosarcina Pasteurii* for Fugitive Dust Control. *Geotech. Spec. Publ.* **2011**, *211*, 4002–4011. [[CrossRef](#)]
29. Duo, L.; Kan-liang, T.; Hui-li, Z.; Yu-yao, W.; Kang-yi, N.; Shi-can, Z. Experimental Investigation of Solidifying Desert Aeolian Sand Using Microbially Induced Calcite Precipitation. *Constr. Build. Mater.* **2018**, *172*, 251–262. [[CrossRef](#)]
30. Nasir, S.S.; Torkashvand, A.M.; Khakipour, N. An Experimental Investigation of Bacteria-Producing Calcareous Cement in Wind Erosion Prevention. *Int. J. Environ. Sci. Technol.* **2021**, *19*, 2107–2118. [[CrossRef](#)]
31. Wang, Z.; Zhang, N.; Ding, J.; Lu, C.; Jin, Y. Experimental Study on Wind Erosion Resistance and Strength of Sands Treated with Microbial-Induced Calcium Carbonate Precipitation. *Adv. Mater. Sci. Eng.* **2018**, *2018*, 3463298. [[CrossRef](#)]
32. Shi, G.; Qi, J.; Wang, Y.; Liu, S. Experimental Study on the Prevention of Coal Mine Dust with Biological Dust Suppressant. *Powder Technol.* **2021**, *391*, 162–172. [[CrossRef](#)]
33. Song, W.; Yang, Y.; Qi, R.; Li, J.; Pan, X. Suppression of Coal Dust by Microbially Induced Carbonate Precipitation Using *Staphylococcus Succinus*. *Environ. Sci. Pollut. Res.* **2019**, *26*, 35968–35977. [[CrossRef](#)]
34. Zhu, S.; Hu, X.; Zhao, Y.; Fan, Y.; Wu, M.; Cheng, W.; Wang, P.; Wang, S. Coal Dust Consolidation Using Calcium Carbonate Precipitation Induced by Treatment with Mixed Cultures of Urease-Producing Bacteria. *Water Air Soil Pollut.* **2020**, *231*, 442. [[CrossRef](#)]
35. Rodin, S.; Champagne, P.; Mann, V. Pilot-Scale Feasibility Study for the Stabilization of Coal Tailings via Microbially Induced Calcite Precipitation. *Environ. Sci. Pollut. Res.* **2022**, *30*, 8868–8882. [[CrossRef](#)] [[PubMed](#)]
36. Wang, C.; Harbottle, D.; Liu, Q.; Xu, Z. Current State of Fine Mineral Tailings Treatment: A Critical Review on Theory and Practice. *Miner. Eng.* **2014**, *58*, 113–131. [[CrossRef](#)]
37. Achal, V.; Pan, X. Influence of Calcium Sources on Microbially Induced Calcium Carbonate Precipitation by *Bacillus Sp. CR2*. *Appl. Biochem. Biotechnol.* **2014**, *173*, 307–317. [[CrossRef](#)] [[PubMed](#)]
38. Gorakhki, M.H.; Bareither, C.A. Unconfined Compressive Strength of Synthetic and Natural Mine Tailings Amended with Fly Ash and Cement. *J. Geotech. Geoenviron. Eng.* **2017**, *143*, 04017017. [[CrossRef](#)]
39. Gorakhki, M.H.; Bareither, C.A. Compressibility Behavior of Synthetic Mine Tailings Amended with Fly Ash. *Geo-Chicago* **2016**, *270*, 255–266.
40. Hamdan, N.; Zhao, Z.; Mujica, M.; Kavazanjian, E.; He, X. Hydrogel-Assisted Enzyme-Induced Carbonate Mineral Precipitation. *J. Mater. Civ. Eng.* **2016**, *28*, 04016089. [[CrossRef](#)]
41. D422-63; Standard Test Method for Particle-Size Analysis of Soils. ASTM International: West Conshohocken, PA, USA, 2007.
42. D4972-19; Standard Test Methods for PH of Soils. ASTM International: West Conshohocken, PA, USA, 2019.
43. D854-14; Standard Test Methods for Specific Gravity of Soil Solids by Water Pycnometer. ASTM International: West Conshohocken, PA, USA, 2016.
44. D2434-22; Standard Test Methods for Measurement of Hydraulic Conductivity of Coarse-Grained Soils. ASTM international: West Conshohocken, PA, USA, 2022.
45. Eltarahony, M.; Zaki, S.; Abd-El-Haleem, D. Aerobic and Anaerobic Removal of Lead and Mercury via Calcium Carbonate Precipitation Mediated by Statistically Optimized Nitrate Reductases. *Sci. Rep.* **2020**, *10*, 4029. [[CrossRef](#)] [[PubMed](#)]
46. Cheng, L.; Cord-ruwisch, R. In Situ Soil Cementation with Ureolytic Bacteria by Surface Percolation. *Ecol. Eng.* **2012**, *42*, 64–72. [[CrossRef](#)]
47. Gomez, M.G.; Anderson, C.M.; Graddy, C.M.R.; DeJong, J.T.; Nelson, D.C.; Ginn, T.R. Large-Scale Comparison of Bioaugmentation and Biostimulation Approaches for Biocementation of Sands. *J. Geotech. Geoenviron. Eng.* **2017**, *143*, 04016124. [[CrossRef](#)]
48. Venuleo, S.; Laloui, L.; Terzis, D.; Hueckel, T.; Hassan, M. Microbially Induced Calcite Precipitation Effect on Soil Thermal Conductivity. *Geotech. Lett.* **2016**, *6*, 39–44. [[CrossRef](#)]
49. Wang, Z.; Zhang, N.; Ding, J.; Li, Q.; Xu, J. Thermal Conductivity of Sands Treated with Microbially Induced Calcite Precipitation (MICP) and Model Prediction. *Int. J. Heat Mass Transf.* **2020**, *147*, 118899. [[CrossRef](#)]
50. Achal, V.; Mukherjee, A.; Basu, P.C.; Reddy, M.S. Strain Improvement of *Sporosarcina Pasteurii* for Enhanced Urease and Calcite Production. *J. Ind. Microbiol. Biotechnol.* **2009**, *36*, 981–988. [[CrossRef](#)]
51. APHA. *Standard Methods for the Examination of Water and Wastewater*; Bridgewater, B.R., Eaton, A.D., Ricé, E.W., Eds.; APHA: Washington, DC, USA, 2017.
52. Khanjani, M.; Westenberg, D.J.; Kumar, A.; Ma, H. Tuning Polymorphs and Morphology of Microbially Induced Calcium Carbonate: Controlling Factors and Underlying Mechanisms. *ACS Omega* **2021**, *6*, 11988–12003. [[CrossRef](#)]
53. Katebi, H.; Fahmi, A.; Ouria, A.; Amini, A.B.; Kafil, H.S. Microbial Surface Treatment of Sand with *Sporosarcina Pasteurii* to Improve the Wind Erosion Resistance in Urmia Lake. *Appl. Environ. Soil Sci.* **2021**, *2021*, 8893115. [[CrossRef](#)]
54. Burbank, M.B.; Weaver, T.J.; Green, T.L.; Williams, B.; Crawford, R.L. Precipitation of Calcite by Indigenous Microorganisms to Strengthen Liquefiable Soils. *Geomicrobiol. J.* **2011**, *28*, 301–312. [[CrossRef](#)]

55. Bu, C.; Wen, K.; Liu, S.; Ogbonnaya, U.; Li, L. Development of Bio-Cemented Constructional Materials through Microbial Induced Calcite Precipitation. *Mater. Struct.* **2018**, *51*, 30. [[CrossRef](#)]
56. Phillips, A.J.; Gerlach, R.; Lauchnor, E.; Mitchell, A.C.; Cunningham, A.B.; Spangler, L. Engineered Applications of Ureolytic Biomineralization: A Review. *Biofouling* **2013**, *29*, 715–733. [[CrossRef](#)]
57. Oliveira, P.J.V.; Neves, J.P.G. Effect of Organic Matter Content on Enzymatic Biocementation Process Applied to Coarse-Grained Soils. *J. Mater. Civ. Eng.* **2019**, *31*, 04019121. [[CrossRef](#)]
58. Coates, J. Interpretation of Infrared Spectra, A Practical Approach. *Encycl. Anal. Chem.* **2006**, *12*, 10815–10837. [[CrossRef](#)]
59. Oliver, K.V.; Maréchal, A.; Rich, P.R. Effects of the Hydration State on the Mid-Infrared Spectra of Urea and Creatinine in Relation to Urine Analyses. *Appl. Spectroscopy* **2016**, *70*, 983–994. [[CrossRef](#)] [[PubMed](#)]
60. Timón, V.; Maté, B.; Herrero, V.J.; Tanarro, I. Infrared Spectra of Amorphous and Crystalline Urea Ices. *Phys. Chem. Chem. Phys.* **2021**, *23*, 22344–22351. [[CrossRef](#)]
61. Chaurasia, L.; Bisht, V.; Singh, L.P.; Gupta, S. A Novel Approach of Biomineralization for Improving Micro and Macro-Properties of Concrete. *Constr. Build. Mater.* **2019**, *195*, 340–351. [[CrossRef](#)]
62. Firdous, R.; Hirsch, T.; Klimm, D.; Lothenbach, B.; Stephan, D. Reaction of Calcium Carbonate Minerals in Sodium Silicate Solution and Its Role in Alkali-Activated Systems. *Miner. Eng.* **2021**, *165*, 106849. [[CrossRef](#)]
63. Gebauer, D.; Gunawidjaja, P.N.; Ko, J.Y.P.; Bacsik, Z.; Aziz, B.; Liu, L.; Hu, Y.; Bergström, L.; Tai, C.W.; Sham, T.K.; et al. Proto-Calcite and Proto-Vaterite in Amorphous Calcium Carbonates. *Angew. Chem. Int. Ed.* **2010**, *49*, 8889–8891. [[CrossRef](#)]
64. Khouzani, M.F.; Chevrier, D.M.; Güttlein, P.; Hauser, K.; Zhang, P.; Hedin, N.; Gebauer, D. Disordered Amorphous Calcium Carbonate from Direct Precipitation. *CrystEngComm* **2015**, *17*, 4842–4849. [[CrossRef](#)]
65. Rodriguez-Blanco, J.D.; Shaw, S.; Benning, L.G. The Kinetics and Mechanisms of Amorphous Calcium Carbonate (ACC) Crystallization to Calcite, Via Vaterite. *Nanoscale* **2011**, *3*, 265–271. [[CrossRef](#)]
66. Krzmann, M.M.; Valant, M.; Jancar, B.; Suvorov, D. Sub-Solidus Synthesis and Microwave Dielectric Characterization of Plagioclase Feldspars. *J. Am. Ceram. Soc.* **2005**, *88*, 2472–2479. [[CrossRef](#)]

**Disclaimer/Publisher’s Note:** The statements, opinions and data contained in all publications are solely those of the individual author(s) and contributor(s) and not of MDPI and/or the editor(s). MDPI and/or the editor(s) disclaim responsibility for any injury to people or property resulting from any ideas, methods, instructions or products referred to in the content.